

Subunit rotation of ATP synthase embedded in membranes: α or β subunit rotation relative to the c subunit ring

Kazuaki Nishio*, Atsuko Iwamoto-Kihara*, Akitsugu Yamamoto†, Yoh Wada*, and Masamitsu Futai**

*Division of Biological Sciences, Institute of Scientific and Industrial Research, Osaka University, Core Research for Evolutional Science and Technology (CREST) of the Japan Science and Technology Corporation, Osaka 567-0047, Japan; and †Department of Physiology, Kansai Medical University, Moriguchi, Osaka 570-8506, Japan

Edited by Paul D. Boyer, University of California, Los Angeles, CA, and approved August 15, 2002 (received for review March 13, 2002)

ATP synthase F_0F_1 ($\alpha_3\beta_3\gamma\delta\epsilon ab_2c_{10-14}$) couples an electrochemical proton gradient and a chemical reaction through the rotation of its subunit assembly. In this study, we engineered F_0F_1 to examine the rotation of the catalytic F_1 β or membrane sector F_0 a subunit when the F_0 c subunit ring was immobilized; a biotin-tag was introduced onto the β or a subunit, and a His-tag onto the c subunit ring. Membrane fragments were obtained from *Escherichia coli* cells carrying the recombinant plasmid for the engineered F_0F_1 and were immobilized on a glass surface. An actin filament connected to the β or a subunit rotated counterclockwise on the addition of ATP, and generated essentially the same torque as one connected to the c ring of F_0F_1 immobilized through a His-tag linked to the α or β subunit. These results established that the $\gamma\epsilon c_{10-14}$ and $\alpha_3\beta_3\delta ab_2$ complexes are mechanical units of the membrane-embedded enzyme involved in rotational catalysis.

ATP is synthesized in mitochondria, chloroplasts, and bacteria by F_0F_1 (ATP synthase) coupled with an electrochemical proton gradient established through an electron transfer chain (for reviews, see refs. 1–6). The minimal functional F_0F_1 , as seen in *Escherichia coli*, consists of a catalytic F_1 sector ($\alpha_3\beta_3\gamma\delta\epsilon$) and a membrane proton pathway F_0 ($a_1b_2c_{10-14}$), comprising five and three different subunits, respectively. The γ subunit occupies the central space of the catalytic $\alpha_3\beta_3$ hexamer and plays essential roles in catalysis and energy coupling, as shown by extensive genetic studies (2, 7–11). The binding change mechanism predicts that the γ subunit interacts alternately with the three β subunits, and the active site in each β subunit catalyzes ATP synthesis or hydrolysis successively (6). Combined genetic and biochemical studies suggested that the γ subunit amino- and carboxyl-terminal domains interact through long-range conformational transmission (9–11). The γ subunit rotation was indicated biochemically by the β/γ cross-linking (12) and movement of a probe covalently connected to the γ subunit (13), and confirmed finally by the continuous rotation of an actin filament connected to the γ subunit of the F_1 sector immobilized on a glass surface (14, 15). As discussed (15), proton transport through F_0 should drive γ rotation, leading to the β subunit conformational change that releases the product ATP. Reversibly, ATP hydrolysis should also drive γ rotation, which is transmitted to the F_0 sector for proton translocation. Thus, the close interaction between the γ subunit and the F_0 sector is pertinent in energy coupling.

Early low-resolution structural analyses involving electron (16) and atomic force microscopy (17, 18) of the F_0 sector suggested that the c subunits form a ring structure, and that other subunits (ab_2) are located outside this ring. A c ring formed from 12 c subunits was proposed on the basis of the solution structure of a monomer (19, 20) and the function of fused multiple copies of the c subunits (21, 22). The yeast x-ray structure indicated that the 10 c monomers form a ring that is tightly associated with the γ subunit (23). A ring structure of different copies was observed more recently on atomic force microscopy (24, 25). Consistent

with the association of the γ subunit and the c ring, Sambongi *et al.* (26) and Pänke *et al.* (27) showed that the c ring rotated continuously together with the γ subunit when F_0F_1 was immobilized on a glass surface through the α or β subunit. We showed that the $\alpha_3\beta_3$ hexamer rotated as well when the c ring was immobilized (28), indicating that the $\epsilon\gamma c_{10-14}$ complex rotates relative to the $\alpha_3\beta_3$ hexamer. A similar result was obtained by another group (unpublished, but cited in ref. 29). These results suggest that $\gamma\epsilon c_{10-14}$ and $ab_2\alpha_3\beta_3\delta$ are an interchangeable rotor and stator, respectively (30, 31). However, continuous rotation of the c ring relative to the a subunit should be directly shown to confirm the rotary mechanism. Furthermore, it would also be desirable to show the rotation of F_0F_1 in membranes because its original integrity is maintained.

In this study, we immobilized membrane fragments on a glass surface through a His-tag introduced onto the c ring and examined the rotation of an actin filament connected to the β subunit. On the addition of ATP, we observed filament rotation, indicating that the β subunit rotated relative to the c ring in membrane-bound F_0F_1 . We further extended this approach to the subunit rotation in the F_0 sector, connecting a filament to the a subunit in a membrane immobilized through the c ring. The a subunit rotated continuously after ATP addition, indicating that the c and a subunits are parts of the interchangeable rotor and stator, respectively.

Experimental Procedures

Plasmids, Bacterial Strain, and Growth Conditions. A plasmid (pBWU13) carrying all *E. coli* F_0F_1 genes (32) was engineered for rotation of the a or β subunit. Glu-2 of the c subunit was replaced by His (CAT) to introduce an *Eco*T22I site (ATGCAT). By using this site, the cassette for His₆-Leu-His was introduced after Met-1 of the c subunit gene. The transcarboxylase biotin-binding domain (Lys-20–Leu-124) (PinPoint Xa-1, Promega) was connected to the β or a subunit. The DNA segment for the biotin-tag with *Kpn*I sites at both termini was introduced between Met-1 and Ala-2 codon of the β subunit gene (into the introduced *Kpn*I site). Similarly, DNA fragment for the biotin-tag with three Glu₄-Ser repeats at the amino terminus was connected to the carboxyl terminus of the a subunit gene. Recombinant plasmids were introduced into *E. coli* strain DK8 (Δunc) lacking the F_0F_1 genes. The bacterium was grown in a synthetic medium containing glycerol and 2 μ M biotin (28).

Membrane Preparation. One gram of cells (late-logarithmic phase) was suspended at 4°C in 10 ml of buffer A [50 mM Tris-HCl (pH 8.0)/0.5 mM EDTA/2 mM MgCl₂/1 mM DTT/10% (wt/vol) glycerol] and disrupted by passage through a French press (1,200

This paper was submitted directly (Track II) to the PNAS office.

Abbreviation: DCCD, *N,N'*-dicyclohexylcarbodiimide.

*To whom correspondence should be addressed. E-mail: m-futai@sanken.osaka-u.ac.jp.

kg/cm²). The lysate was centrifuged at 20,000 × *g* for 10 min, and the supernatant was centrifuged again under the same conditions. The supernatant was carefully withdrawn and was centrifuged at 200,000 × *g* (average) for 80 min. The precipitate was suspended in 7 ml of buffer A, and then the centrifugation was repeated. The resulting precipitate was suspended in ≈0.5 ml of buffer A to give ≈30 mg of protein per ml, rapidly frozen in liquid nitrogen, and stored at −80°C until use. Cells were disrupted under higher pressure and the membranes were obtained under different centrifugation conditions from those usually used for preparing everted vesicles: the pressure used for previous studies was 400 kg/cm² (33).

Immobilization of Membranes and Observation of Rotation. A flow cell (≈0.1 mm deep; ≈11 mm³ volume) was constructed from nitrocellulose-coated cover glass, filled with buffer B (10 mM Hepes–NaOH, pH 7.8/25 mM KCl/6 mM MgCl₂) containing 0.8 μM Ni²⁺-nitrilotriacetate–horseradish peroxidase conjugate (Qiagen, Hilden, Germany) and incubated for 5 min (15). The flow cell was washed with buffer B containing 10 mg/ml BSA, and incubated for 5 min. Membranes were rapidly thawed in 37°C water bath, diluted 30- to 60-fold at 25°C in buffer B (final protein concentration of 0.5–1 mg/ml) and introduced into the flow cell. The following procedures were performed at 25°C. After incubation for 10 min, 20 μl of 12 μM streptavidin in buffer B containing BSA was introduced. After incubation for 5 min, the flow cell was washed with 150 μl of the same buffer and then 50 mM Tris·HCl (pH 7.8) containing 12 nM fluorescent actin filaments was introduced. Immediately after introduction of 50 μl of reaction mixture for rotation (without an ATP-regenerating system) (15), a 1-mm² area was scanned under a Zeiss Axiovert 135 with an intensified charge-coupled device camera, and the rotating filaments were video-recorded and analyzed as described (15, 26, 28, 34).

Other Procedures. ATPase activity and protein concentrations were determined as described (32). Fluorescent biotinylated actin filaments were prepared by the published procedure (15). Membrane preparations were studied by electron microscopy as described (35). Immunogold conjugate EM streptavidin was from BB International (Cardiff, U.K.). All other materials used were of the highest grade commercially available.

Results and Discussion

Preparation of Membranes with Engineered F_oF₁. Recombinant plasmids for two types of engineered F_oF₁ were constructed after introducing a His-tag onto the *c* subunit: (Fig. 1*a*) a biotin-tag on the β subunit; and (Fig. 1*b*) a biotin-tag together with a linker on the *a* subunit. They were introduced into *E. coli* DK8 cells lacking the genes for ATP synthase. The strain harboring either plasmid could grow on succinate by oxidative phosphorylation slightly slower than that with the control plasmid (pBWU13) encoding the wild-type nonengineered F_oF₁. The ATPase activities of membranes with engineered F_oF₁ were 15–20% of those with the wild-type nonengineered F_oF₁. These results were possibly due to the low specific activities and reduced amounts of the engineered enzymes, because Western blotting with anti-β-subunit antibodies gave less dense bands for membranes with an engineered F_oF₁ (Fig. 2, lanes 1–3). In this regard, the lower ATPase activity of the purified F_oF₁ with a His-tag connected to the *c* ring and a biotin-tag connected to the β subunit was shown previously (28). It should be noted that the engineered membrane enzyme was sensitive to dicyclohexylcarbodiimide (DCCD), similar to the wild type (Table 1).

Membranes with a biotin-tag on the β and *a* subunits gave single bands on gel electrophoresis as judged when Western blotting was performed with streptavidin (Fig. 2, lanes 4–6). These bands correspond to increased molecular weights (60,000

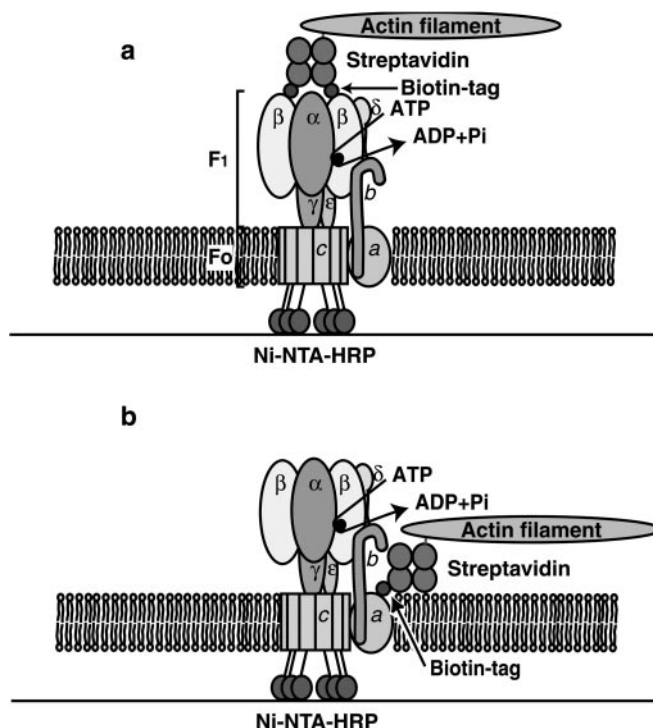


Fig. 1. Experimental systems for observing the rotation of filaments connected to the β or *a* subunit in membrane-embedded F_oF₁. His- and biotin-tags were introduced onto the *c* and β (*a*) or *a* (*b*) subunits, respectively. Membranes were immobilized on a glass surface through a His-tag, and an actin filament was connected to the β or *a* subunit through a biotin-tag and streptavidin. Ni-NTA-HRP, Ni²⁺-nitrilotriacetate–horseradish peroxidase.

and 43,000, respectively) because of the connection of the 105-aa biotin-tag. On the other hand, the control membranes (wild type with nonengineered F_oF₁) did not give any band (Fig. 2, lane 6), indicating that no protein reactive with streptavidin was present. Thus, only the subunits with a biotin-tag could bind to streptavidin and the actin filament for rotation observation described below.

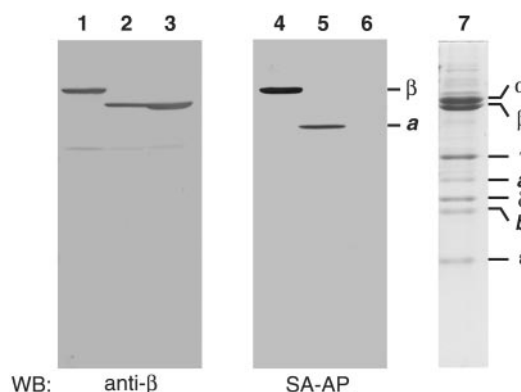


Fig. 2. Gel electrophoresis of membranes with engineered F_oF₁. Membranes (10 μg of protein) with engineered F_oF₁ were subjected to 12.5% polyacrylamide gel electrophoresis in the presence of SDS, and then subjected to Western blotting (WB) with anti-β-subunit antibodies; lane 1, cHis-tag/β biotin-tag; lane 2, cHis-tag/*a* biotin-tag; lane 3, nonengineered wild-type. The nitrocellulose membrane was also blotted with streptavidin-alkaline phosphatase conjugate (SA-AP): lane 4, cHis-tag/β biotin-tag enzyme; lane 5, cHis-tag/*a* biotin-tag enzyme; lane 6, nonengineered wild-type. Purified non-engineered F_oF₁ was applied and stained with Coomassie brilliant blue as markers (lane 7).

Table 1. Properties of membranes with F_oF₁ engineered for rotation

Membranes with F _o F ₁	Growth on succinate	Membrane ATPase, units/mg protein	DCCD inhibition, %
Nonengineered	+++	14.0	80
cHis-tag/ β biotin-tag	++	3.7	70
cHis-tag/ α biotin-tag	++	2.2	72

Growth by oxidative phosphorylation was estimated: cells were grown at 37°C on a succinate plate for 2 days. Membranes (10 μ g of protein per ml) were incubated in 0.05 M Tris-HCl, pH 8.0, at 25°C for 10 min in the absence and presence of various concentrations of DCCD and then their ATPase activities were determined. Inhibition with 50 μ M DCCD is shown.

Properties of Membranes Exhibiting Subunit Rotation. We previously purified F_oF₁ with a His-tag on the *c* ring and a biotin-tag on the α or β subunit (28), which were immobilized and connected with an actin filament. On the addition of ATP, the filaments rotated continuously and generated essentially the same frictional torque as those connected to the *c* ring of the purified F_oF₁ (26). Because the His- and biotin-tags faced the periplasm and cytoplasm, respectively, the planar plasma membrane fragments could be immobilized on a glass surface, and used for analyzing the rotation. On the other hand, we expected that everted membrane vesicles could not bind to the glass surface because the His-tag was located inside. Right-side-out vesicles could be immobilized from the His-tag outside. However, they could not bind actin filaments because the biotin-tag is located inside the vesicles. Thus, only the planar membrane fragment could be immobilized on the glass surface and bind actin filament (Fig. 1).

From these considerations, we decided to test membranes prepared by differential centrifugation after disrupting cells by French press. This procedure has been used for preparation of everted vesicles (33, 36–37). However, presence of planar membranes in the preparation could be expected from the low rate of oxidative phosphorylation (P/O ratio) of membranes prepared by disrupting cells even by using low pressure (37). We obtained a better membrane preparation for rotation by passing cells through a French press with slight modification of the procedure used for everted vesicle preparation (32).

Because the biotin-tag was introduced into the β subunit, we could label membranes with streptavidin-conjugated gold particles similar to labeling them with an actin filament for rotation. The membrane preparation contained a significant number of planar fragments; electron microscopy after the negative staining showed that about 80% of the total population attaching the gold particles was the fragments (apparently not vesicles) (Fig. 3*a*). The rest of the population was vesicles surrounded by bilayers. They were everted vesicles because their F₁ could bind gold particles and could not be immobilized on a glass surface, as discussed above. Membranes without biotin-tag in the β subunit bound much fewer particles (\approx 3% of those with the tag), indicating the specific binding to the tag. We also immobilized membranes on the glass surface under the conditions for rotation experiments, fixed them, and embedded them into the resin. Electron microscopy of the sections showed that gold particles were attached mostly to the membrane fragment (Fig. 3*b*). These results suggest that membrane preparation contains planar membranes that could attach gold particles.

Rotation of an Actin Filament Connected to the β Subunit in Membranes. Membranes were immobilized on a glass surface and the actin filament was connected by using essentially the same procedure as for the purified engineered F_oF₁. Actin filament connected to the β subunit in membrane rotated counterclockwise after the addition of ATP (Fig. 4*a*). Ten to 16 rotating filaments were observed when we scanned a 2.0-mm² area. No

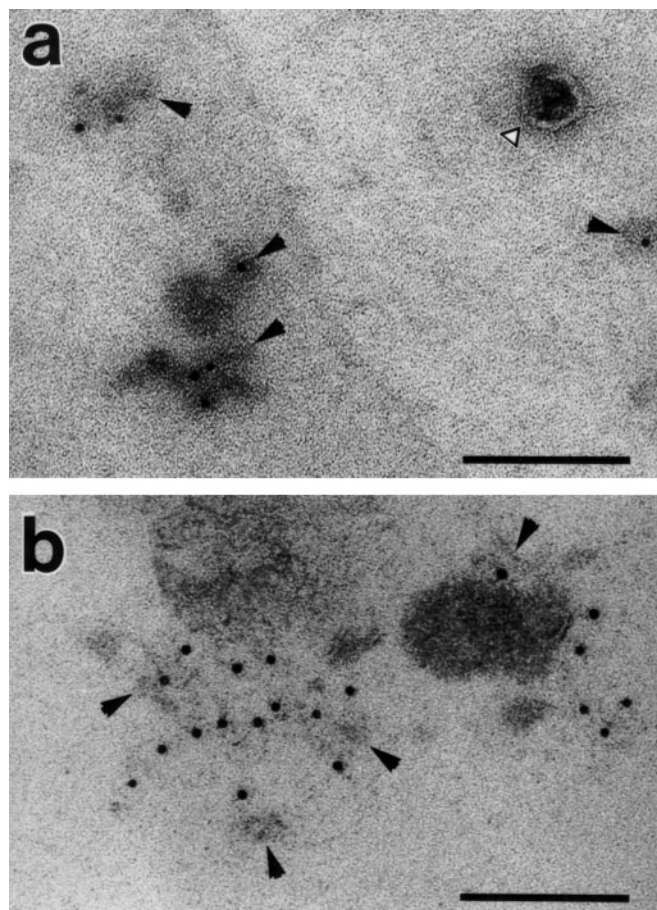


Fig. 3. Engineered membranes used for testing rotation. (*a*) Electron microscopy of negatively stained membranes. Membranes with cHis-tag/ β biotin-tag enzyme in buffer A (14 mg of protein per ml) were applied to a copper grid coated with polyvinyl formal, incubated with streptavidin gold (1.7×10^{11} particles per ml) in PBS containing 0.5% BSA, and washed extensively with 0.1 M cacodylate buffer (pH 7.4). They were fixed with 2.5% glutaraldehyde and stained with 0.3% uranyl acetate. Membranes observed are filled arrowhead, fragment with gold particle; open arrowhead, vesicle. (Scale bar, 100 nm.) We counted the number of gold particles attached to membrane fragments and vesicles, and found 865 and 259, respectively, in a 360- μ m² area. The gold particles bound to membranes without biotin-tag were \approx 3% of those with the tag. (*b*) Electron microscopy of membranes immobilized for rotation experiments. Membranes with cHis-tag/ β biotin-tag enzyme were immobilized on the glass surface and reacted with streptavidin gold particles under essentially the same conditions for rotational assay. They were fixed with 2.5% glutaraldehyde and subsequently 1% OsO₄ and were embedded in Epon. After careful removal of the glass, the embedded sample was sectioned (0.5° to the original glass surface), and sections were observed under an electron microscope after staining with 2% uranyl acetate followed by Reynold's lead citrate. Essentially the same results were obtained for membranes with cHis-tag/ α biotin-tag enzyme. Examples of membrane fragment with gold particles are shown by filled arrowheads. (Scale bar, 100 nm.)

rotating filaments were observed in the following controls with F₁ or membranes: (*i*) purified F₁ with a biotin-tag on the β subunit (no His-tag on the γ subunit); (*ii*) the same F₁ mixed with a mutant (DK8) membrane lacking F_oF₁; (*iii*) membranes with biotin-tag to the β subunit but without His-tag. These controls apparently could not attach to the glass surface because F₁ is not associated with membranes, or membranes lacked a His-tag. Thus, contaminating F₁, if any, was not responsible for the rotation observed. These results suggest that an experimental system was established for observing the subunit rotation of F_oF₁ in membranes.

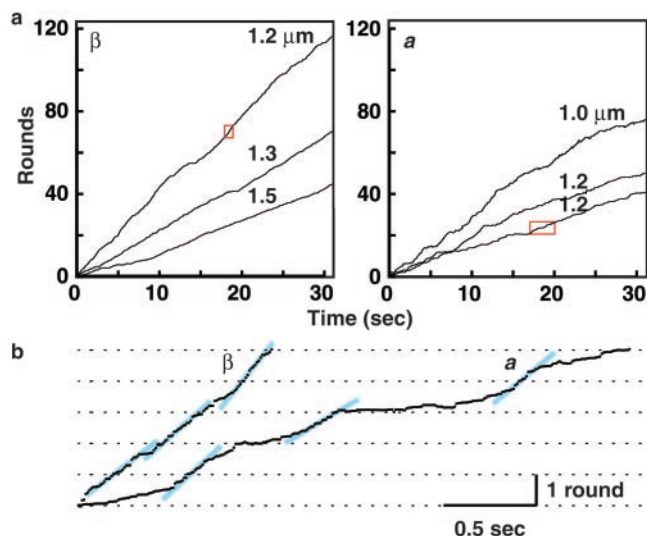


Fig. 4. Rotation of an actin filament connected to the a or β subunit of F_0F_1 embedded in membranes. (a) Time courses of rotation of actin filaments connected to the β or a subunit. Rotating filaments (1–1.5 μm) were video-recorded and the resulting images were analyzed (26). The filaments rotated continuously counterclockwise, as viewed from the F_1 side. (b) Expanded time courses of rotating actin filaments. The boxed areas in a (for 1.2- μm filaments) are expanded as examples for estimating rotational rates (light blue straight lines).

Rotation of an Actin Filament Connected to the a Subunit in Membranes. The observation of β subunit rotation in membranes prompted us to analyze the relative rotation of the a and c subunits. An actin filament connected to the a subunit in the membrane F_0F_1 rotated counterclockwise after ATP addition (Fig. 4a). The rotating filaments found amounted to 10–20% of those connected to the β subunit. The a subunit rotation was less smooth than that of the β subunit, possibly because the probe connected to the a subunit may be closer to the membrane surface than that connected to the β subunit. Consistent with this interpretation, a biotin-tag attached directly to the a subunit carboxyl terminus could not bind to an actin filament, indicating that the spacer in front of the biotin-tag is essential for obtaining membrane F_0F_1 capable of rotation. We could not observe rotation with the membrane F_0F_1 having a biotin-tag on the a subunit but lacking a His-tag on the c ring, indicating that the c ring should be anchored to the glass surface by a His-tag. These results clearly show that the a subunit can rotate in membranes relative to the c ring.

Properties of the Rotation of Membrane F_0F_1 . Actin filaments connected to membrane F_0F_1 rotated less smoothly than ones attached to the purified F_1 (15) or F_0F_1 (26, 28) (Fig. 4a). This tendency was more apparent for the a than the β rotation. We expanded the time scale, and found a higher frequency of pausing in the membrane subunit rotation (Fig. 4a). These results suggest that the actin filament rotation may be affected by other proteins localized in the same membranes. We thus calculated rotational rates after expanding the time scale (Fig. 4b) and plotted the results against viscous drag. As shown in Fig. 5, the a and β subunit rotation generated essentially the same frictional torque (≈ 40 pN-nm) as that observed for the purified F_0F_1 or F_1 .

The rotation of an actin filament connected to the c ring was sensitive to venturicidin when the purified F_0F_1 was immobilized on a glass surface through a His-tag on the α or β subunit (26, 28). On the other hand, the rotation and ATPase activity of the purified F_0F_1 (c His-tag/ β biotin-tag) were not inhibited by

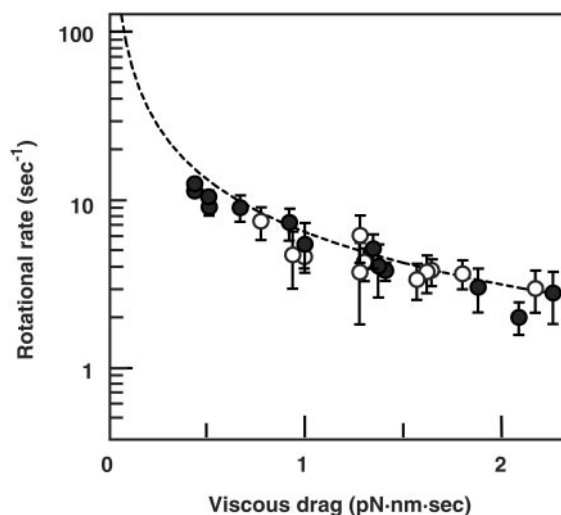


Fig. 5. Frictional torque generated by membrane F_0F_1 rotation. The rates of rotation of actin filaments connected to the β (○) and a (●) subunits were obtained as shown in Fig. 4b, and are plotted against viscous drag. Calculation of the drag was performed as described (34). The dotted line represents the calculated rate, assuming a constant torque of 40 pN-nm.

venturicidin (28), suggesting that the introduction of a His-tag onto the c subunit affects the inhibitor binding. As expected from these previous observations, the rotation in a membrane with a c His-tag were not sensitive to venturicidin (data not shown).

Because F_0F_1 showed low sensitivity to DCCD in the buffer used for rotation (28), its effect on the rotational filament was not easy to study. The difficulties in testing this inhibitor have been extensively discussed (28, 30). It should be remembered that DCCD is not effective right after its addition to the reaction mixture, and it does not cause complete inhibition of F_0F_1 or membrane ATPase (for example, see ref. 28). Therefore, we

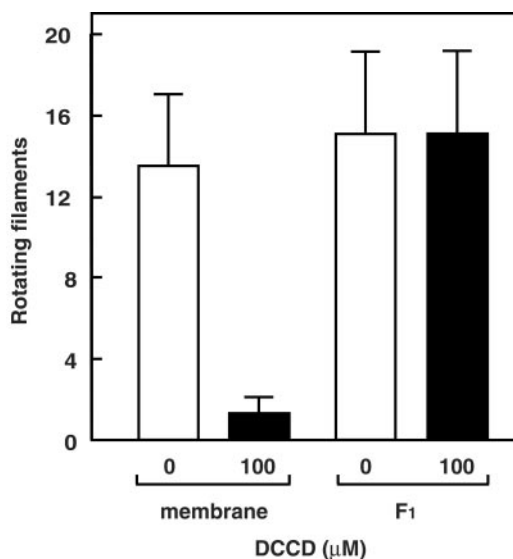


Fig. 6. Effects of DCCD on rotation of filaments connected to the β subunit. Membranes (1 mg/ml) were treated with 100 μM DCCD at 25°C for 10 min in 10 mM Hepes-NaOH, pH 7.8, containing 25 mM KCl and 6 mM MgCl_2 and immobilized on a glass surface, and then actin filaments were connected and their rotation was examined. After the addition of ATP, a 2-mm² area was rapidly scanned to find rotating filaments. The numbers of rotating filaments are shown with the standard deviations. Open bars, control without DCCD treatment; filled bars, with DCCD.

could not examine the inhibition by directly adding DCCD to the rotating filaments under the microscope. Considering these limitations, we incubated membranes with DCCD at pH 7.8 in the presence of MgCl_2 (Fig. 6, legend) and then examined them for filament rotation. This condition is for DCCD binding to the c subunit, not to the β subunit of the F_1 sector (38). The filaments rotating in DCCD-treated membranes amounted to about 1/10 of those nontreated (Fig. 6). On the other hand, no effect of DCCD was observed on the rotation of a filament connected to the γ subunit of F_1 . These results indicate that rotation of F_0F_1 in membranes is sensitive to DCCD.

As described above, we observed α or β subunit rotation

relative to the c ring in membrane F_0F_1 . By combining the present results and those obtained with purified F_0F_1 (26–28), we could establish that $\alpha_3\beta_3\delta ab_2$ and $\gamma\epsilon c_{10-14}$ are an interchangeable stator and rotor, respectively. Furthermore, it should be emphasized that the present results were obtained with membrane-embedded F_0F_1 . Thus, our results are free from any effects on F_0F_1 during solubilization and purification with detergent(s).

We thank Dr. Y. Sambongi and Ms. Y. Iko for the helpful discussion and for conducting the blind test on the rotation. We are also grateful to Ms. S. Shimamura and Ms. M. Nakashima for their assistance in preparing the manuscript.

1. Futai, M., Noumi, T. & Maeda, M. (1989) *Annu. Rev. Biochem.* **58**, 111–136.
2. Futai, M. & Omote, H. (1996) in *Handbook of Biological Physics*, eds. Konings, W. N., Kaback, H. R. & Lolkema, J. S. (Elsevier, Amsterdam), Vol. 2, pp. 47–74.
3. Penefsky, H. S. & Cross, R. L. (1991) *Adv. Enzymol. Relat. Areas Mol. Biol.* **64**, 173–214.
4. Weber, J. & Senior, A. E. (1997) *Biochim. Biophys. Acta* **1319**, 19–58.
5. Fillingame, R. H. (1996) *Curr. Opin. Struct. Biol.* **6**, 491–498.
6. Boyer, P. D. (1997) *Annu. Rev. Biochem.* **66**, 717–749.
7. Iwamoto, A., Miki, J., Maeda, M. & Futai, M. (1990) *J. Biol. Chem.* **265**, 5043–5048.
8. Shin, K., Nakamoto, R. K. & Futai, M. (1992) *J. Biol. Chem.* **267**, 20835–20839.
9. Nakamoto, R. K., Maeda, M. & Futai, M. (1993) *J. Biol. Chem.* **268**, 867–872.
10. Nakamoto, R. K. & Futai, M. (1996) *Biomembrane* 343–367.
11. Futai, M. & Omote, H. (1996) *J. Bioenerg. Biomembr.* **28**, 409–414.
12. Duncan, T. M., Bulygin, V. V., Zhou, Y., Hutcheon, M. L. & Cross, R. L. (1995) *Proc. Natl. Acad. Sci. USA* **92**, 10964–10968.
13. Sabbert, D., Engelbrecht, S. & Junge, W. (1996) *Nature* **381**, 623–625.
14. Noji, H., Yasuda, R., Yoshida, N. & Kinosita, K., Jr. (1997) *Nature* **386**, 299–302.
15. Omote, H., Sambonmatsu, N., Saito, K., Sambongi, Y., Iwamoto-Kihara, A., Yanagida, T., Wada, Y. & Futai, M. (1999) *Proc. Natl. Acad. Sci. USA* **96**, 7780–7784.
16. Birken Häger, R., Hoppert, M., Deckers-Hebestreit, G., Mayer, F. & Altmendorf, K. (1995) *Eur. J. Biochem.* **230**, 58–67.
17. Takeyasu, K., Omote, H., Nettikadan, S., Tokumasu, F., Iwamoto-Kihara, A. & Futai, M. (1996) *FEBS Lett.* **392**, 110–113.
18. Singh, S., Turina, P., Bustamante, J. C., Keller, J. D. & Capaldi, R. (1996) *FEBS Lett.* **397**, 30–34.
19. Dmitriev, O. Y., Jones, P. C. & Fillingame, R. H. (1999) *Proc. Natl. Acad. Sci. USA* **96**, 7785–7790.
20. Rastogi, V. K. & Girvin, M. E. (1999) *Nature* **402**, 263–268.
21. Jones, P. C. & Fillingame, R. H. (1998) *J. Biol. Chem.* **273**, 29701–29705.
22. Fillingame, R. H., Jiang, W., Dmitriev, O. Y. & Jones, P. C. (2000) *Biochim. Biophys. Acta* **1458**, 387–403.
23. Stock, D., Leslie, A. G. W. & Walker, J. E. (1999) *Science* **286**, 1700–1705.
24. Seelert, H., Poeth, A., Dencher, N. A., Engel, A., Stahlberg, H. & Müller, D. J. (2000) *Nature* **405**, 418–419.
25. Müller, D. J., Dencher, N. A., Meiser, T., Dimroth, P., Suda, K., Stahlberg, H., Engel, A., Seelert, H. & Matthey, U. (2001) *FEBS Lett.* **504**, 219–222.
26. Sambongi, Y., Iko, Y., Tanabe, M., Omote, H., Iwamoto-Kihara, A., Ueda, I., Yanagida, T., Wada, Y. & Futai, M. (1999) *Science* **286**, 1722–1724.
27. Pänke, O., Gumbiowski, K., Junge, W. & Engelbrecht, S. (2000) *FEBS Lett.* **472**, 34–38.
28. Tanabe, M., Nishio, K., Iko, Y., Sambongi, Y., Iwamoto-Kihara, A., Omote, H., Wada, Y. & Futai, M. (2001) *J. Biol. Chem.* **276**, 15269–15274.
29. Junge, W., Pänke, O., Cherepanov, D. A., Gumbiowski, K., Müller, M. & Engelbrecht, S. (2001) *FEBS Lett.* **504**, 152–160.
30. Wada, Y., Sambongi, Y. & Futai, M. (2000) *Biochim. Biophys. Acta* **1459**, 499–505.
31. Sambongi, Y., Ueda, I., Wada, Y. & Futai, M. (2000) *J. Bioenerg. Biomembr.* **32**, 441–448.
32. Moriyama, Y., Iwamoto, A., Hanada, H., Maeda, M. & Futai, M. (1991) *J. Biol. Chem.* **266**, 22141–22146.
33. Kanazawa, H., Miki, T., Tamura, F., Yura, T. & Futai, M. (1979) *Proc. Natl. Acad. Sci. USA* **76**, 1126–1130.
34. Iko, Y., Sambongi, Y., Tanabe, M., Iwamoto-Kihara, A., Saito, K., Ueda, I., Wada, Y. & Futai, M. (2001) *J. Biol. Chem.* **276**, 47508–47511.
35. Yamato, I., Futai, M., Anraku, Y. & Nonomura, Y. (1978) *J. Biochem. (Tokyo)* **83**, 117–128.
36. Futai, M. (1974) *J. Membr. Biol.* **15**, 15–28.
37. Hertzberg, E. L. & Hinkle, P. C. (1974) *Biochem. Biophys. Res. Commun.* **58**, 178–184.
38. Yoshida, M., Allison, W. S., Esch, F. S. & Futai, M. (1982) *J. Biol. Chem.* **257**, 10033–10037.